Novel Numerical Dissipation Scheme for Level-Set Based Anisotropic Etching Simulations

Alexander Toifl
Christian Doppler Laboratory for High Performance TCAD
Institute for Microelectronics, TU Wien
Wien, Austria
toifl@iue.tuwien.ac.at

Michael Quell
Christian Doppler Laboratory for High Performance TCAD
Institute for Microelectronics, TU Wien
Wien, Austria
quell@iue.tuwien.ac.at

Andreas Hössinger
Silvaco Europe Ltd.
Cambridge, United Kingdom
andreas.hoessinger@silvaco.com

Artem Babayan
Silvaco Europe Ltd.
Cambridge, United Kingdom
artem.babayan@silvaco.com

Siegfried Selberherr
Institute for Microelectronics, TU Wien
Wien, Austria
selberherr@tuwien.ac.at

Josef Weinbub
Christian Doppler Laboratory for High Performance TCAD
Institute for Microelectronics,TU Wien
Wien, Austria
weinbub@iue.tuwien.ac.at

***Abstract*—We propose a novel dissipation scheme for level-set based wet etching simulations. The scheme enables modeling of the temporal evolution of the etch profile during anisotropic wet etching processes and is based on the local geometry and the crystallographic direction-dependent etch rate. We implemented the scheme into Silvaco's Victory Process simulator which is utilized in this work to simulate the fabrication of source/drain cavities for sub-28 nm strained metal-oxide-semiconductor field-effect transistors. Our results show excellent agreement with experimental data. In particular, the main cavity-related design variables are accurately predicted.**

I. Introduction

Anisotropic etching of silicon (Si) with wet etchants (e.g., potassium hydroxide (KOH) and tetramethylammonium hydroxide (TMAH)) is an important processing technique which utilizes the crystalline nature of the material. While KOH etching is mainly known for its application in the production of micro-electro-mechanical-systems (MEMS) [1], TMAH etching plays an important role for embedded silicon germanium (e-SiGe) in source/drain (S/D) engineered sub-$28\,\mathrm{nm}$ node metal-oxide-semiconductor field-effect transistors (MOSFETs) [2], [3]. By employing a combination of dry and wet etching a S/D cavity formed by the characteristic $\{111\}$-planes can be produced. The exact geometry of the resulting sigma-shaped cavity determines the uniaxial strain in the MOSFET channel after epitaxial growth of SiGe [4]. Thus, it is very important to control the critical design variables, i.e., tip depth, channel-cavity distance, and cavity depth [2].

In this work we present a dissipation scheme for level-set based simulations of anisotropic wet etching, which allows to predict the temporal evolution during the etching step and the final profile with high accuracy. The proposed scheme was implemented into Silvaco's Victory Process simulator [5], which we utilize to simulate the process steps required for sigma-shaped cavities for S/D engineering.

II. Etch Rate Modeling Within the Level-Set Framework

We employ the level-set method [6], [7] [8], where the wafer surface is described by the zero level-set of the function ϕ and the time evolution is determined by the level-set equation

$$\frac{\partial \phi}{\partial t} + H(\nabla \phi) = 0. \tag{1}$$

The level-set equation assumes the form of a Hamiltonian-Jacobi equation with the corresponding Hamiltonian $H = V(\nabla\phi)|\nabla\phi|$. The speed function V is constructed to reflect the highly anisotropic etch rates. We assume constant process temperature and neglect the influence of reactant transport on the etching kinetics. Under these conditions, the etch rate depends on the crystallographic planes which are exposed to the surface resulting in the self-limited etch profiles observed in experiments [1]. Consequently, we model V to assume the form

$$V = V(n^x, n^y, n^z) = V(\nabla\phi), \tag{2}$$

which is a function of the components n^l, $l \in \{x, y, z\}$ of the level-set normal vector $n = \nabla\phi/|\nabla\phi|$. The etch rates along the main crystal directions are well known from experiments. In order to define a continuous speed function, we use linear interpolation between a set of crystal directions, e.g., $\langle 100\rangle$, $\langle 110\rangle$, and $\langle 111\rangle$ with their associated etch rates R_{100}, R_{110}, and R_{111}, respectively, while taking the cubic symmetry of silicon into account [9], [10]. Fig. 1 illustrates that the resulting speed function is spatially strongly varying. As a consequence, the resulting Hamiltonian is non-convex, which detrimentally impacts the stability of the numerical solution of the level-set equation [8].

978-1-7281-0940-4/19/$31.00

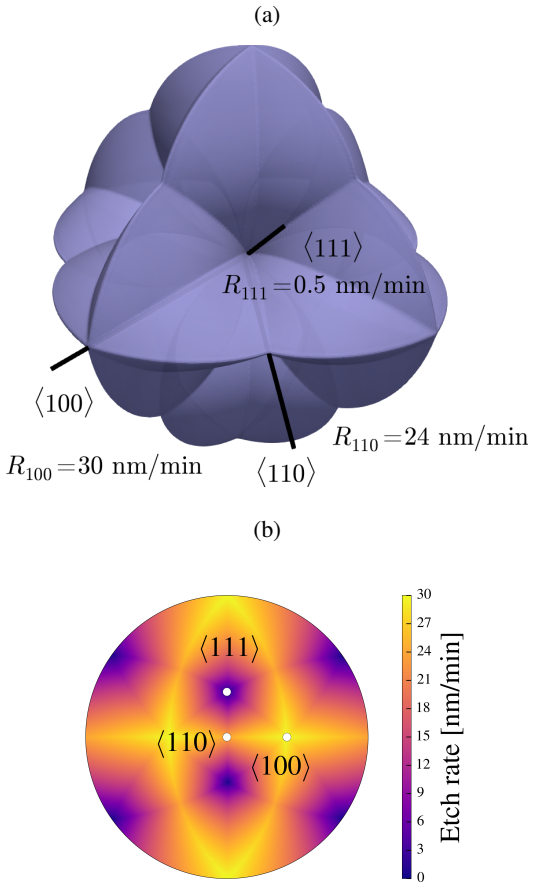

Fig. 1: The etch rate distribution function which originates from a linear interpolation between silicon's main crystallographic directions ⟨100⟩, ⟨110⟩, and ⟨111⟩ is visualized in a **(a)** three dimensional and **(b)** stereographic plot. The highly anisotropic etch rate distribution is typical for wet etchants [11] and is presented here for a TMAH solution (40 °C, 2.38 wt%) as given by *Qin et al.* [3].

A non-convex Hamiltonian is problematic for wet etching simulations, because the front is typically characterized by sharp corners, resulting in regions of high curvature. In particular, a non-convex speed function $V(n)$ (illustrated in the inset) assigns the level-set grid points along a high curvature front strongly varying speed values, as depicted in Fig. 2. The limited resolution invoked by the spatial discretization gives rise to the problem that the speed of the front between two grid points can only be estimated by some kind of combination of the values at exactly these two grid points, causing instable front propagation [12].

III. Dissipation Scheme

In order to enable a stable and physically relevant numerical solution, the dissipative Lax-Friedrichs scheme [13], [15] is employed. The time integration is performed with the (first-

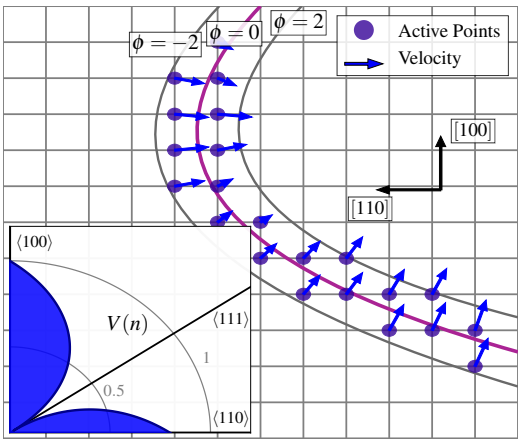

Fig. 2: The highly anisotropic etch rates in Fig. 1 give rise to spatially strongly varying velocities assigned to the level-set normals and a non-convex Hamiltonian. The level-set normals are shown for active grid points, which reside within the narrow band $|\phi| < 2.0$. The inset illustrates the speed function $V(n)$ in the depicted plane, which is characterized by a global minimum along ⟨111⟩ directions and two maxima.

order) Euler method. Associated with the Lax-Friedrichs-Scheme is the *numerical* Hamiltonian $\hat{H}$

$$\hat{H} = H\left(\frac{\phi_l^- + \phi_l^+}{2}\right) - \sum_l \alpha^l \left(\frac{\phi_l^+ - \phi_l^-}{2}\right), \qquad (3)$$

where ϕ_l^-, ϕ_l^+, $l \in \{x, y, z\}$ denote backward and forward differences of ϕ with respect to l. The Lax-Friedrichs scheme critically depends on the dissipation coefficients α^l which define the numerical dissipation (viscosity) $\sum_l \alpha^l \left(\phi_l^+ - \phi_l^-\right)/2$. The numerical dissipation has to be chosen appropriately to enable a stable and consistent surface evolution and to avoid artificially rounded corners. Consequently, for the particular case of wet etching it is essential to find a trade-off between accurate undercut rates and sharp corners formed by the slowly moving crystal planes.

In contrast to former approaches [14], [15] [16] we employ a novel *local* approach based on a stencil S (Fig. 3), which considers the processed and neighboring grid points P. In particular, the stencil integrates information about the local geometry and the *nature* of $V(n^x, n^y, n^z)$.

$$\alpha^l = \max_{P \in S} \Gamma \left| \frac{\partial V}{\partial n^l} \frac{\phi_p^2 + \phi_q^2}{|\nabla\phi|^2} - \frac{\partial V}{\partial n^p} \frac{\phi_p \phi_l}{|\nabla\phi|^2} - \frac{\partial V}{\partial n^q} \frac{\phi_q \phi_l}{|\nabla\phi|^2} + V n^l \right|$$
$$l, p, q \in \{x, y, z\},\ l \neq p \neq q \qquad (4)$$

$\Gamma > 0$ denotes an etchant-specific prefactor which is treated as a calibration parameter. $\partial V / \partial n^l$ is numerically evaluated using central differences

$$\frac{\partial V}{\partial n^x} = \frac{V(n^x + \Delta N, n^y, n^z) - V(n^x - \Delta N, n^y, n^z)}{2\Delta N} \qquad (5)$$

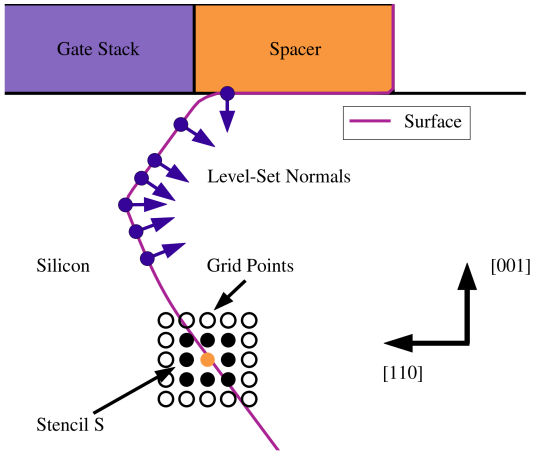

Fig. 3: The proposed dissipation scheme (4) is based on normals and the associated speed functions which are calculated for a stencil consisting of the central grid point and its immediate neighbors.

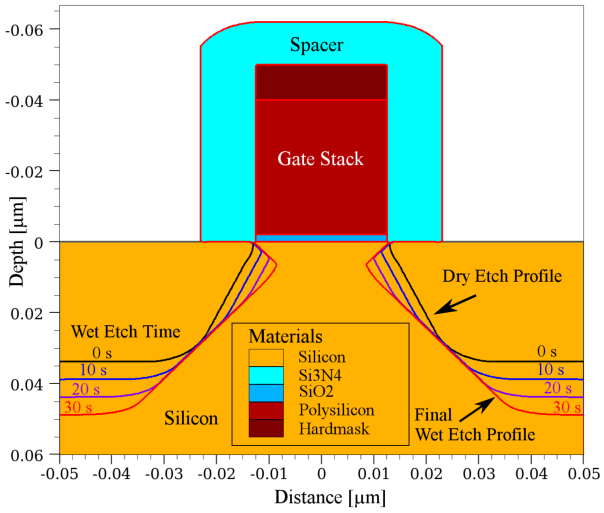

Fig. 4: Temporal evolution of the etch profile. During the self-limiting wet etching the slow-moving $\{111\}$ planes form the sigma-shaped cavity.

and analogous expressions for the remaining spatial coordinates with $\Delta N = 10^{-6}$. The expression for the dissipation coefficients (4) originates from monotonicity considerations, which are based on the Lax-Friedrichs scheme being a monotone scheme [13]. Employing (4), the stencil Lax-Friedrichs scheme (3) introduces the appropriate amount of numerical dissipation at the mask-silicon interface and enables the prediction of the correct mask undercut rate.

IV. Simulation Results and Discussion

The proposed dissipation scheme is applied to simulate the sigma-cavity process presented by Qin *et al.* [3], which is based on a two-step reactive ion etching (RIE) step and a sequential wet etching step. The RIE step is split into an anisotropic and isotropic sub-step in order to optimize the initial condition ('Dry Etch Profile' in Fig. 4) for a 30 s wet etch using a TMAH solution (40 °C, 2.38 wt%).

The fabrication of the sigma-cavities has been simulated with Silvaco's Victory Process simulator, including gate stack and spacer formation. In order to demonstrate the viability of the proposed dissipation scheme, we emulate a two-step RIE process (anisotropic and ideal isotropic step) to provide the initial profile depicted in Fig. 5. The proposed dissipation scheme has been utilized for the subsequent wet etching step with the speed function V (three-rate linear interpolation) defined by the rates along the high-symmetry planes $R_{100} = 30\,\mathrm{nm/min}$, $R_{110} = 24\,\mathrm{nm/min}$, and $R_{111} = 0.5\,\mathrm{nm/min}$ (Fig. 1).

The level-set equation is considered on a regular grid with a spatial resolution $\Delta x = \Delta y = 0.5\,\mathrm{nm}$. The dissipation coefficients (4) are calculated for all points residing in the narrow band, which is defined as the set of grid points with an associated level-set value satisfying $|\phi| < 2.0$. Within the narrow band all grid points hold a valid velocity value, which is strongly related to the surface velocity by extending the surface values to the respective grid points (velocity extension) [7]. Furthermore, we use $\Gamma = 3.0$ for the TMAH solution as a calibration parameter.

Fig. 4 visualizes the temporal evolution to the final profile, where the dry etch profile and the etch profile are shown after 10 s, 20 s, and 30 s. Due to the characteristically small etch rate of $\{111\}$ planes, the final profile consists of two $\{111\}$ planes which define a sharp corner at a certain position relative to the channel (sigma-cavity tip). The associated design parameters tip depth D and channel-cavity distance δ are depicted in Fig. 5, where the experimentally obtained etch profiles presented by Qin *et al.* [3] are compared to the simulation results. The wet etching simulations accurately reproduce D, δ, and the cavity depth. The dissipation scheme does not introduce non-physical rounding at the point of contact of the resulting two $\{111\}$ planes.

Furthermore, we assess our dissipation scheme by performing the same process simulation steps with the elementary dissipation coefficients, which are computed purely based on the local speed function and level-set normal [7].

$$\alpha^l = \max_{P \in S} \left| V n^l \right|, \quad l \in \{x, y, z\} \tag{6}$$

The elementary dissipation coefficients give rise to insufficient dissipation beneath the spacer and gate stack, which leads to an artificially high undercut rate and consequently to an incorrect sigma tip position. In particular, with respect to the experimental observations, the elementary scheme results in a displaced sigma tip position by 1.6 nm in x-direction and 4.2 nm in y-direction, which is significantly higher than the spatial resolution $\Delta x = 0.5\,\mathrm{nm}$ and thus not acceptable. In contrast, the proposed scheme (4) reproduces the physical undercut and is able to predict the geometry of the sigma-shaped cavity with high accuracy.

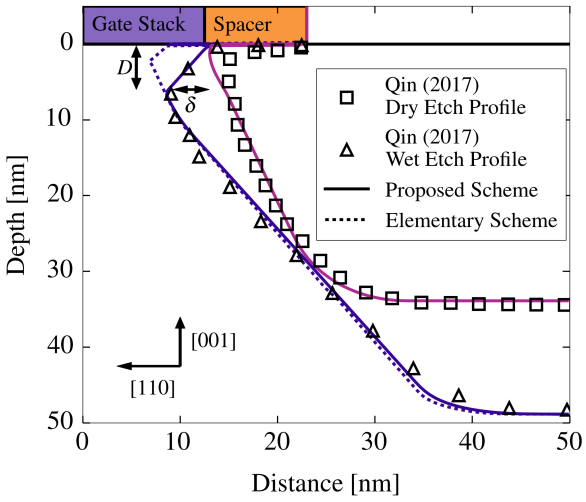

Fig. 5: The etch profiles presented by Qin *et al.* [3] are accurately reproduced using the proposed scheme (4). In contrast, the elementary scheme (6) starting from the same dry etch profile results in artificially high undercut.

V. Summary

We have proposed a novel dissipation scheme for level-set based simulations of anisotropic wet etching processes. The scheme is based on the Lax-Friedrichs approach and is optimized for purely surface normal-dependent speed functions, which excellently model the etching kinetics of common etchants (e.g., TMAH and KOH). We have employed the dissipation scheme to accurately predict the sigma S/D cavity profiles for sub-28 nm node strained MOSFETs. In particular, the predicted cavity-related design parameters – tip depth, channel-cavity distance, and cavity depth – are shown to match with the experimental observations, while artificial smoothing of sharp corners is avoided.

Acknowledgment

The financial support by the *Austrian Federal Ministry for Digital and Economic Affairs* and the *National Foundation for Research, Technology and Development* is gratefully acknowledged.

References

[1] H. Geng, *Semiconductor Manufacturing Handbook*. McGraw-Hill Education, 2017.

[2] H. Lo, J. Peng, E. Reis, B. Zhu, W. Ma, S. Y. Mun, S. Shintri, E. M. Bazizi, C. Gaire, Y. Qi, J. Chen, S. N. Ting, O. Hu, and S. Samavedam, "A Novel Approach to Control Source/Drain Cavity Profile for Device Performance Improvement," *IEEE Trans. Electron Devices*, vol. 65, no. 9, pp. 3640–3645, 2018.

[3] C. Qin, H. Yin, G. Wang, P. Hong, X. Ma, H. Cui, Y. Lu, L. Meng, H. Yin, H. Zhong, J. Yan, H. Zhu, Q. Xu, J. Li, C. Zhao, and H. H. Radamson, "Study of Sigma-Shaped Source/Drain Recesses for Embedded-SiGe pMOSFETs," *Microelec. Eng.*, vol. 181, pp. 22–28, 2017.

[4] Y.-Q. Sui, Q.-H. Han, H. Zhang, and K.-F. Lee, "A Study of Sigma-shaped Silicon Trench Formation," *ECS Trans.*, vol. 52, no. 1, pp. 331–335, 2013.

[5] "Silvaco Victory Process," https://www.silvaco.com/products/tcad.html, (accessed June 18, 2019).

[6] J. A. Sethian, "A Fast Marching Level Set Method for Monotonically Advancing Fronts," *Proc. Natl. Acad. Sci.*, vol. 93, pp. 1591–1595, 1996.

[7] S. Osher and R. Fedkiw, *Level Set Methods and Dynamic Implicit Surfaces*. Springer, 2003.

[8] J. A. Sethian, "Evolution, Implementation, and Application of Level Set and Fast Marching Methods for Advancing Fronts," *J. Comput. Phys.*, vol. 169, no. 2, pp. 503–555, 2001.

[9] T. J. Hubbard, "MEMS Design: The Geometry of Silicon Micromachining," Ph.D. dissertation, California Institute of Technology, 1994.

[10] B. Radjenović, J. K. Lee, and M. Radmilović-Radjenović, "Sparse Field Level Set Method for Non-Convex Hamiltonians in 3D Plasma Etching Profile Simulations," *Comput. Phys. Commun.*, vol. 174, no. 2, pp. 127–132, 2006.

[11] M. Gosálvez, P. Pal, and K. Sato, "Reconstructing the 3D Etch Rate Distribution of Silicon in Anisotropic Etchants Using Data From Vicinal {1 0 0}, {1 1 0} and {1 1 1} surfaces," *J. Micromech. Microeng.*, vol. 21, no. 10, p. 105018, 2011.

[12] J. A. Sethian and D. Adalsteinsson, "An Overview of Level Set Methods for Etching, Deposition, and Lithography Development," *IEEE Trans. Semicond. Manuf.*, vol. 10, no. 1, pp. 167–184, Feb 1997.

[13] B. M. G. Crandall and P. L. Lions, "Two Approximations of Solutions of Hamilton-Jacobi Equations," *Math. Comput.*, vol. 43, no. 167, pp. 1–19, 1984.

[14] C. Montoliu, N. Ferrando, M. A. Gosálvez, J. Cerdá, and R. J. Colom, "Implementation and Evaluation of the Level Set Method: Towards Efficient and Accurate Simulation of Wet Etching for Microengineering Applications," *Comput. Phys. Commun.*, vol. 184, no. 10, pp. 2299–2309, 2013.

[15] C. Montoliu, N. Ferrando, M. A. Gosálvez, J. Cerdá, and R. J. Colom, "Level Set Implementation for the Simulation of Anisotropic Etching: Application to Complex MEMS Micromachining," *J. Micromech. Microeng.*, vol. 23, no. 7, pp. 1–17, 2013.

[16] B. Radjenović and M. Radmilović-Radjenović, "3D Simulations of the Profile Evolution During Anisotropic Wet Etching of Silicon," *Thin Solid Films*, vol. 517, no. 14, pp. 4233–4237, 2009.